

Modifications to the Water Vapor Continuum in the Microwave Suggested by Ground-Based 150-GHz Observations

David D. Turner, Maria P. Cadetdu, Ulrich Löhnert, Susanne Crewell, *Member, IEEE*, and Andrew M. Vogelmann

Abstract—Ground-based observations from two different radiometers are used to evaluate commonly used microwave/millimeter-wave propagation models at 150 GHz. This frequency has strong sensitivity to changes in precipitable water vapor (PWV) and cloud liquid water. The observations were collected near Hesselbach, Germany, as part of the Atmospheric Radiation Measurement program's support of the General Observing Period and the Convective and Orographic Precipitation Study. The observations from the two radiometers agree well with each other, with a slope of 0.993 and a mean bias of 0.12 K. The observations demonstrate that the relative sensitivity of the different absorption models to PWV in clear-sky conditions at 150 GHz is significant and that four models differ significantly from the observed brightness temperature. These models were modified to get agreement with the 150-GHz observations, where the PWV ranged from 0.35 to 2.88 cm. The models were modified by adjusting the strength of the foreign- and self-broadened water vapor continuum coefficients, where the magnitude was model dependent. In all cases, the adjustment to the two components of the water vapor continuum was in opposite directions (i.e., increasing the contribution from the foreign-broadened component while decreasing contribution from the self-broadened component or vice versa). While the original models had significant disagreements relative to each other, the resulting modified models show much better agreement relative to each other throughout the microwave spectrum. The modified models were evaluated using independent observations at 31.4 GHz.

Index Terms—Atmospheric measurements, microwave measurements, microwave propagation, microwave radiometry, remote sensing.

Manuscript received November 7, 2008; revised March 13, 2009 and April 16, 2009. First published July 7, 2009; current version published September 29, 2009. This work was supported in part by the Environmental Sciences Division, Office of Biological and Environmental Research, Office of Science, U.S. Department of Energy, as part of the ARM program under Grant DE-FG02-06ER64167 to the University of Wisconsin–Madison and Grant B&R KP1205010 to Brookhaven National Laboratory and in part by the German Research Foundation under Grant WU356/4-2 to the University of Cologne.

D. D. Turner is with the Space Science and Engineering Center, University of Wisconsin–Madison, Madison, WI 53706 USA (e-mail: dtuner@ssec.wisc.edu).

M. P. Cadetdu is with the Argonne National Laboratory, Argonne, IL 60439 USA.

U. Löhnert and S. Crewell are with the Institute of Geophysics and Meteorology, University of Cologne, 50923 Cologne, Germany.

A. M. Vogelmann is with the Atmospheric Sciences Division, Brookhaven National Laboratory, Upton, NY 11973 USA.

Color versions of one or more of the figures in this paper are available online at <http://ieeexplore.ieee.org>.

Digital Object Identifier 10.1109/TGRS.2009.2022262

I. INTRODUCTION

RADIATIVE transfer (RT) models are used to compute the propagation of radiant energy through various media. Accurate RT models, particularly in the visible and infrared wavelength regimes, are needed to improve our understanding of atmospheric processes and to capture the radiative impact of these processes in numerical models such as global climate models. Furthermore, RT models in all spectral regions are an important component of any remote sensing technique.

RT models need to account for the scattering of radiation by particles, as well as the emission and absorption by both particles and gases. In order to properly account for the radiative contribution of gases, many RT models use the spectral absorption parameters (e.g., line position, strength, half width, and temperature dependence) that are available in common spectral databases (e.g., HITRAN [1]). However, as the assumed line shapes used in RT models are not perfect, there are contributions in the far wings of these absorption lines that are accounted for in most RT models with a “continuum” absorption model. Improving the accuracy of these continuum absorption models, particularly those associated with water vapor absorption, has been an ongoing challenge for the RT community.

Microwave and millimeter-wave (henceforth, “microwave”) observations of the atmosphere have a tremendous amount of information regarding the temperature and humidity structure of the atmosphere, as well as the total amount of water vapor and cloud liquid in the column (e.g., [2]–[9]). Furthermore, airborne and satellite microwave remote sensors provide information about the surface, including emissivity and moisture content (e.g., [10]–[12]). These applications require accurate RT models to prevent biases from affecting the results.

The scientific community has used several different microwave RT models for these applications. There have been numerous comparisons of different microwave RT models relative to each other and to observations (e.g., [13]–[16]). Many of these comparisons have been limited to frequencies below 60 GHz, but there have been a few studies that evaluated the accuracy of microwave RT models at higher frequencies. For example, Racette *et al.* [17] used observations from multiple radiometers in the Arctic to evaluate three different models up to 340 GHz; however, the maximum amount of precipitable water vapor (PWV) in this study was less than 0.6 cm, and there was significant uncertainty in the PWV. Hewison [18] used airborne microwave radiometer observations collected in conditions ranging from the Arctic to the tropics to evaluate

different RT models from 89 to 183 GHz; in this case, the 33 profiles were all measured by the aircraft that also carried the five-channel radiometer used in the comparison. These studies suggest a need for additional validation of the microwave absorption models at higher frequencies. This is particularly important as several current and future satellite sensors make observations at higher frequencies such as 90 and 150 GHz (e.g., Advanced Microwave Sounding Unit).

The Atmospheric Radiation Measurement (ARM) program, in support of the Convective and Orographically Induced Precipitation Study [19] and the long-term model evaluation of the General Observing Period [20], deployed the ARM Mobile Facility (AMF, [21]) to the Black Forest region in southwestern Germany from April through December 2007. The AMF was situated in the middle of the Murg Valley (48.54° N, 8.41° E) to provide data that could be used to help improve the quantitative forecasting of precipitation, including the diurnal cycle and windward/lee effect of the mountains. This valley location resulted in frequent fog and dew formation events, particularly during calm evenings, and was frequently cloudy during the day due to the orographic forcing and convective activity. Nonetheless, many cloud-free periods with coincident radiosonde launches were identified during this nine-month AMF deployment, which were used in our clear-sky evaluation.

We have used these clear-sky periods to evaluate the accuracy of different commonly used microwave RT models. Our results suggest that modifications should be made to the strength of the water vapor continuum absorption parameterizations used by all of these models in order to get better agreement with the 150- and 31.4-GHz observations.

II. INSTRUMENTATION

The AMF instrument complement includes the routine launching of Vaisala RS92 radiosondes (four/day), a two-channel microwave radiometer (23.8 and 31.4 GHz), micropulse lidar, infrared interferometer, and other instruments. The AMF was augmented with two additional radiometers that make observations of the downwelling radiance at 90 and 150 GHz. Liquid water absorbs more strongly at these higher frequencies than in the 20–30-GHz range, and thus, observations at these higher frequencies can significantly improve the accuracy of the retrieved liquid water path (LWP) [22]. Accurate LWP is important in order to determine the radiative properties of liquid water clouds (e.g., [23]). However, there is a limit to the improvement in the retrieved LWP that can be achieved with these larger frequencies when the LWP gets large, as the brightness temperature may saturate at these frequencies for clouds with large LWP. We used these high-frequency observations to evaluate four commonly used microwave RT models in cloud-free scenes, which is the first step in incorporating these frequencies into cloud property retrieval algorithms.

The observations used in this analysis were collected by two radiometers manufactured by Radiometer Physics GmbH (RPG). The first radiometer, which is owned by the ARM program and will henceforth be called the microwave radiometer–high frequency (“MWRHF”), is a two-channel system that makes observations at 90 and 150 GHz. The sec-

ond radiometer, which is the Dual Polarization Radiometer (DPR) owned by the University of Munich and fielded by the University of Cologne, is a three-channel system that also makes observations at 90 and 150 GHz. A wire grid is used to separate the polarizations at the latter frequency, so that both the vertical and horizontal polarizations can be measured separately and simultaneously. RPG has incorporated many features from their lower frequency multiwavelength radiometers into these radiometers, including excellent thermal stability (e.g., the temperature of the radio-frequency deck is maintained within 30 mK) [24]. Both radiometers use direct detection at 90 GHz, whereas the 150-GHz channels are heterodyne systems. The newer MWRHF employs a highly stable internal noise source for frequent (once every second) updates of the radiometer sensitivity (gain). For the DPR, the gain is only updated every few minutes by interrupting the atmospheric observations and viewing an internal blackbody target at ambient temperature.

Both radiometers were also occasionally calibrated by viewing a liquid-nitrogen target, and the observations from this target and the internal blackbody are used to determine the noise source temperature, system noise temperature, and the gain. Since the noise source and the system noise temperature are assumed to be highly stable, RPG recommends liquid-nitrogen calibration at the beginning of a deployment and every few months after that. This calibration method requires an operator to install the calibration target on the radiometer and fill it with liquid nitrogen. While the liquid-nitrogen calibration principle for both radiometers is similar, the realization is quite different. The DPR is a scanning instrument that is mounted on a rotating horizontal axis. The liquid-nitrogen calibration target is placed under the DPR, and the entire radiometer is rotated around its horizontal axis to view this target; the rotation of the entire instrument is done to preserve the polarization of the incoming radiation. For the MWRHF system, the liquid-nitrogen calibration target is mounted on one side of the radiometer, the elevation mirror is directed toward that side, and an aluminum reflector is used to redirect the radiation from the target into the instrument. The liquid-nitrogen calibrations for both radiometers were carried out by different operators and at different times. Therefore, the liquid-nitrogen calibration of the two radiometers can be considered to be largely independent of each other; however, it is possible that both radiometers may have common systematic errors because the calibration approach is similar, resulting in an underestimate of the radiometric calibration uncertainty.

The instruments also performed regularly scheduled tip scans [25], which were automatically evaluated by the operational software on the radiometers to update the calibration if the sky was determined to be homogeneous and cloud free. For both radiometers, the calibration of the 90-GHz channels was updated many times between liquid-nitrogen calibration events; however, due to the opacity and variability of the atmosphere at 150 GHz, all of the tip-scan calibrations were considered to be invalid, and thus, none was applied. Therefore, the calibrations of the 150-GHz data from both the MWRHF and DPR were determined solely from the liquid-nitrogen calibrations, while the calibration of the 90-GHz observations included a mixture of liquid-nitrogen and tip-scan calibrations. A postanalysis of

the 90-GHz tip calibration periods determined that many of these periods were not valid due to fog and dew accumulation on the radomes of the radiometers, and thus, the calibration of the 90-GHz data was neither constant nor accurate over time. Unfortunately, due to the lack of some of the essential housekeeping fields in both instruments' data sets, the 90-GHz data cannot be reprocessed to restore the calibration of this channel with confidence. Thus, our analysis here has focused purely on the 150-GHz observations.

Each of the instruments is able to maintain the calibration determined from the liquid-nitrogen views by regularly viewing the internal ambient blackbody target, which has the same design for both the DPR and MWRHF. This target, which is constructed of carbon-loaded foam in the shape of pyramids, is hermetically isolated from the environment with transparent low-density foam. The enclosed air inside the blackbody is circulated with small fans, drawing air through the pyramids and by gauged thermometers; these sensors are able to measure the temperature of the air with an absolute accuracy of ± 0.1 K. Regular views of this ambient blackbody (every few minutes) with the stable noise diode on and off are used to monitor the gain of the instrument.

As indicated earlier, the 150-GHz brightness temperature (T_b) observations from the two radiometers were independently calibrated. The DPR was operational at the AMF site from May 2 until October 5, 2007, when it was removed from the site to support a different experiment. The MWRHF was still under construction at the start of the AMF deployment and thus was sent directly from the RPG factory to the AMF site. It started operation on June 22, although a liquid-nitrogen calibration was not performed until June 30. The MWRHF operated until the end of December 2007, when the AMF concluded operations in the Murg Valley. Both instruments collected only zenith observations during this deployment.

The two radiometers were simultaneously operational for essentially three months, but there were many periods when dew formed on the radomes and clouds were overhead. We have identified over 2000 coincident samples on 24 different days when the two radiometers were operational, did not have dew on their radomes, and were determined to be cloud free. These samples were selected by ensuring that the standard deviation of the observed T_b was less than 1 K over a 5-min period, the mean T_b was less than 190 K (which corresponds to the T_b of an atmosphere of more than 3.3 cm of PWV), and there were at least 20 observations in the averaging period. The center frequency and bandpass of the 150-GHz channels of both radiometers are essentially identical; thus, a direct comparison of the observations can be made. A comparison of these clear-sky cases (Table I, Fig. 1) demonstrates that the observations at 150 GHz from the two radiometers were in excellent agreement with each other, with a slope of 0.993 K/K, a mean bias of -0.12 K, and a correlation coefficient of 0.998. Therefore, we believe that these observations are accurate and can be used with confidence to evaluate the accuracy of microwave RT models.

We also used brightness temperature observations from the ARM two-channel (23.8 and 31.4 GHz) microwave radiometer system. These two-channel systems are present at all of the ARM sites, providing PWV and LWP retrievals for the program

TABLE I
COMPARISON OF COINCIDENT CLEAR-SKY OBSERVATIONS FROM THE MWRHF AND DPR OBSERVATIONS AT 150 GHz. THE CLEAR-SKY SCENES WERE SELECTED FROM 24 DIFFERENT DAYS

Mean bias	-0.12 K
RMS Difference	1.29 K
Slope	0.993 K/K
Intercept	1.10 K
Correlation	0.998
Number of points	2122

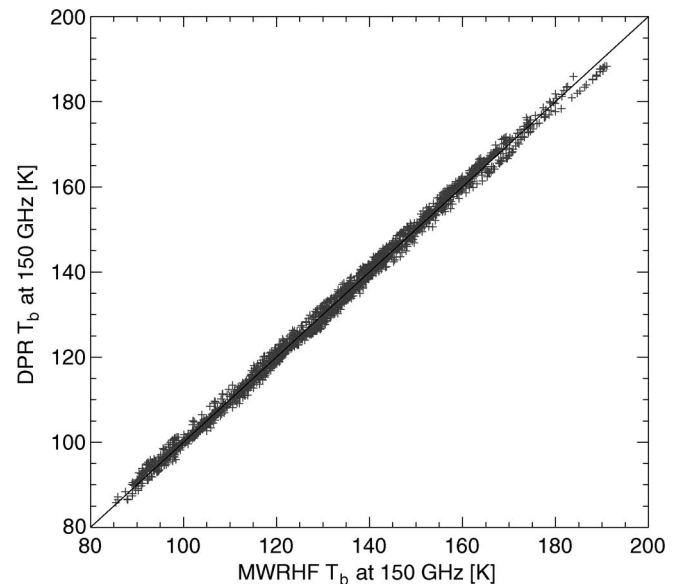


Fig. 1. Comparison of the MWRHF and DPR brightness temperature observations at 150 GHz. Statistics for this comparison are shown in Table I.

for over 15 years, and have been extensively evaluated by many investigators (e.g., [26]). These systems are automatically calibrated with tip scans and use robust data quality checks and thousands of valid tip calibrations, which help to ensure good stable calibration of the radiometer with a root-mean-square (rms) uncertainty in the observed brightness temperatures of approximately 0.3 K [27]. In addition, these two-channel systems are equipped with a heater/blower mechanism that directs warm air over the radome to prevent the formation of dew on the radiometer. Unfortunately, due to manufacturing lead time, heater mechanisms were not added to the DPR and MWRHF systems until after the AMF campaign was over.

III. MODELS

While there are dozens of different microwave absorption models available, we have chosen to evaluate four of the perhaps most commonly used models. These models are the Millimeter-wave Propagation Model ([28]; henceforth called "Liebe87"), which is an updated version of this model ([29]; henceforth called "Liebe93"), a model that uses water vapor continuum components from both of these models with improvements to other aspects of the model ([30] and [31]; henceforth, "Rosen98"), and an independent model used by the ARM program for many years ([32], henceforth called "MonoRTM"). These particular models have been compared extensively with each other at frequencies between 20 and

60 GHz (e.g., [13]–[15]). We used version 3.3 of MonoRTM, which includes the modified half widths of the 22.2- and 183.3-GHz water vapor line [33]. An updated version of MonoRTM (v4.0), released in September 2008, yields very similar results as v3.3 at 150 GHz. Similarly, an updated version of the Rosen98 model (released in 2003) yields essentially identical results to the Rosen98 model at 150 GHz.

The Liebe87, Liebe93, and Rosen98 models only account for the absorption due to water vapor, oxygen, and nitrogen in the microwave. MonoRTM includes contributions from other molecules such as ozone, nitrous oxide, and carbon monoxide, which have only a minor impact on the microwave spectrum at 150 GHz (less than 0.15 K). For this paper, we have specified the concentrations of all gases other than water vapor, oxygen, and nitrogen to be zero in the MonoRTM calculations, thus simplifying the comparison with the other three models. Ignoring the radiative contributions from these trace gases has a negligible impact on the 150 and 31.4 GHz results shown here. Note that all four of the models account for the contribution due to nitrogen, which is approximately 1.6 K (0.8 K) at 150 GHz when the PWV is 0.35 cm (2.88 cm) in a downwelling calculation.

The water vapor continuum absorption parameterization has two components, one accounting for the broadening by foreign gases (e.g., nitrogen and oxygen) and one accounting for the broadening by water vapor. These components, indicated here as α_f and α_s , are referred to as the foreign- and self-broadened components of the water vapor continuum, respectively. The coefficients C_f and C_s are the foreign- and self-broadened water vapor continuum coefficients, respectively.

The formulation of a suitable expression to represent the water vapor continuum has been revised multiple times in the various models. The Liebe93 model uses a modified line shape to account for the absorption in the far wings of the water vapor lines [29] and thus does not use the formalism used by Liebe87, Rosen98, or MonoRTM, which is fairly similar (described as follows). To compare the various formulations and better understand the following results, it is important to review the water vapor continuum used in the Liebe87, Rosen98, and MonoRTM models and to express them in common units. In the Liebe87 and Rosen98 models, the water vapor continuum absorption α [(1), units of decibels per kilometer] is the sum of the foreign- and self-broadened components [(2) and (3), respectively], where the continuum coefficients were determined by fitting experimental data collected at 138 GHz [28], [30], [31]

$$\alpha = \nu^2 \theta^3 (\alpha_f + \alpha_s) \quad (1)$$

$$\alpha_f = C_f \theta^{x_1} P_d P_\nu \quad (2)$$

$$\alpha_s = C_s \theta^{x_2} P_\nu^2 \quad (3)$$

In (1)–(3), P_d is the dry air pressure, P_ν is the partial pressure of water vapor, θ is the normalized temperature (typically 300 K divided by the ambient temperature), and x_1 and x_2 capture the temperature dependence of the foreign- and self-broadened continuum components, respectively. Thus, it can be seen that the α_f term scales linearly with water vapor, while α_s increases with the square of the amount of water vapor. The Rosen98 model uses the C_f value in Liebe87, increased

TABLE II
VALUES OF C_f AND C_s AT 275 K AT 150 GHz FOR THE ORIGINAL ROSEN98, MONORTM, AND LIEBE87 MODELS, ALONG WITH THE TEMPERATURE DEPENDENCE COEFFICIENTS OF THE FOREIGN- AND SELF-BROADENED WATER VAPOR CONTINUUM COEFFICIENTS (x_1 AND x_2 , RESPECTIVELY)

Model	Coefficients (GHz ² kPa ²)		Temperature Dependence Coefs	
	$C_f (x 10^{-9})$	$C_s (x 10^{-7})$	x_1	x_2
Rosen98	5.4	1.8	0.0	4.5
MonoRTM	6.3	1.0	0.0	3.78
Liebe87	4.7	1.95	0.0	7.5 [†]
Liebe93	See Table 5		1.55	4.55

[†]Some versions of Liebe87 use 7.8.

by 15% to account for the different line shape, and the value and temperature dependence of C_s from Liebe93.

MonoRTM (prior to version 4) uses version 2.4 of the Clough–Kneizys–Davies continuum [32], [34]. In this formulation, the total water vapor continuum absorption α (also in decibels per kilometer) is the sum of the foreign- and self-broadened components, where the two components are given by

$$\alpha_f = \nu \tanh\left(\frac{h\nu}{2k_B T}\right) \left(\frac{n - n_\nu}{n_0}\right) n_\nu C_f(\nu) \quad (4)$$

$$\alpha_s = \nu \tanh\left(\frac{h\nu}{2k_B T}\right) \left(\frac{n_\nu}{n_0}\right) n_\nu C_s(T, \nu) \quad (5)$$

where the molecular density n can be expressed as a function of pressure (P) and temperature (T) as $n = 2.415\theta P * 10^{22} \text{ mol} \cdot \text{cm}^{-2} \cdot \text{km}^{-1}$, with $\theta = 300/T$; n_0 is the molecular density at $T = 296 \text{ K}$; and $P = 1 \text{ atm}$. The molecular density of water vapor (n_ν) is computed similarly as n , replacing the atmospheric pressure with the vapor pressure. The water vapor continuum coefficients C_f and C_s are the spectral density functions with units of $(\text{mol} \cdot \text{cm}^{-2} \cdot \text{cm}^{-1})^{-1}$, and only the latter has temperature dependence. The frequency dependence of C_f and C_s in the microwave region is very weak (both change less than 0.5% from 10 to 200 GHz) and therefore can be considered constant. Like the Rosen98 and Liebe87 models ((1)–(3)), α_f depends linearly on water vapor (as $n - n_\nu$ is the dry air density), and α_s depends on the square of the water vapor abundance. In addition, in the microwave region, the radiation field term $\nu \tanh(h\nu/2k_B T)$ can be approximated by $h\nu^2/2k_B T$, where h and k_B are the Planck and Boltzmann constants, respectively. After substituting these expressions in (4) and (5) and converting wavenumbers (cm^{-1}) to frequency (in gigahertz), the MonoRTM formulation can be written in the same form as (1)–(3) with the only difference being the weak frequency dependence of C_f and C_s .

Finally, the Rosen98, Liebe87, and MonoRTM models have no temperature dependence in the foreign continuum ($x_1 = 0$), while the Liebe93 model does assume a temperature dependence on C_f (Table II). On the other hand, MonoRTM, Liebe93, and Rosen98 models have a similar temperature dependence for the self-broadened continuum, while the Liebe87 model assigns much stronger temperature dependence to this term. Some versions of the Liebe87 model have $x_2 = 7.8$; however, this change has negligible influence on these results.

It is clear that, at a given frequency and a given temperature, the Rosen98, Liebe87, and MonoRTM water vapor continuum

formulations differ by multiplicative factors that determine the relative strengths of the self and foreign contributions. In Table II, we show the values of C_f and C_s and the temperature dependence coefficients for the Liebe87, Rosen98, and MonoRTM models. Given the different temperature dependences of the models, the coefficients in the table have been computed at $T = 275$ K, which is the mean water-vapor-weighted temperature for the 71 profiles used in this analysis.

IV. WATER VAPOR SPECIFICATION

Profiles of water vapor and temperature are needed as input to these microwave RT models. Many programs, including the ARM program, rely heavily on radiosondes to specify the temperature and humidity structure of the atmosphere. The ARM program launches radiosondes manufactured by Vaisala at all of its Climate Research Facilities, including the AMF. Extensive studies have been performed using various models of Vaisala radiosondes at the ARM facilities and elsewhere. These studies have shown that there is variability in the calibration of the humidity sensor of these radiosondes that can be corrected, to first order, by multiplying the observed water vapor mixing ratio by a height-independent scale factor [35]. This “PWV scale factor” is derived as the ratio of the PWV retrieved from the two-channel microwave radiometer and the integrated water vapor from the original radiosonde profile [36], [37]. This approach also mitigates a significant diurnal variability in the radiosonde humidity measurement [37], where the daytime dry bias is induced by solar radiative heating of the humidity sensor [38].

We have selected 71 cases for this analysis, where a case consists of a coincident observation from either the DPR or MWRHF and a radiosonde launch. The 150-GHz observations were screened to ensure that dew was not present on the radiometer and that the sky was cloud free. This screening was done using observations from a combination of instruments, including surface meteorology, backscatter profiles from a micropulse lidar, and radiance observations from an infrared interferometer which has excellent sensitivity to small amounts of liquid water [39]. This screening resulted in 23 nighttime and 48 daytime cases, where cases were classified as “daytime” if they had solar zenith angles less than 88° . The integrated water vapor from the radiosondes for these 71 cases ranged from 0.37 to 2.76 cm, with a mean value of 1.54 cm.

We derived PWV scale factors for each of the radiosonde humidity profiles used in this analysis by retrieving PWV from the 23.8-GHz channel of the two-channel ARM microwave radiometers. We decided to only use this frequency in the physical retrieval because of the following: 1) This spectral location is essentially independent of the assumed half width of the 22.2-GHz line and 2) this channel is less sensitive to uncertainties in the water vapor continuum than the 31.4-GHz channel. This also allows the 31.4-GHz observations to be used as an independent check on our analysis later. However, Turner *et al.* [40] have determined that a bias offset needs to be determined and removed from the observation at 23.8 GHz before the PWV can be retrieved.

The bias offset at 23.8 GHz was determined using the approach outlined in [40]. We first computed the mean and

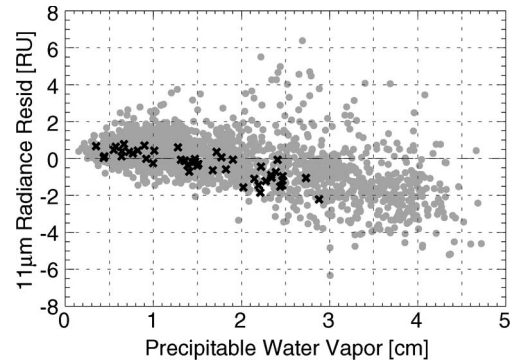


Fig. 2. AERI-observed minus LBLRTM-calculated clear-sky radiance residuals at 900 cm^{-1} ($11.1\ \mu\text{m}$) as a function of PWV. The ARM SGP site data are shown with gray dots, while the data from the AMF deployment to the Murg Valley are shown in black crosses. A radiance unit is $1\text{ mW}/(\text{m}^2 \cdot \text{sr} \cdot \text{cm}^{-1})$.

standard deviation of the 23.8- and 31.4-GHz T_b observations in a 40-min window centered at each nighttime radiosonde launch time during the entire deployment. A T_b -dependent threshold test applied to the standard deviation of the 31.4-GHz observations [40] identified 94 nighttime clear-sky cases. The MonoRTM was then used to compute the T_b at 23.8 GHz for these clear-sky radiosondes, where the radiosondes were scaled with a height-independent scale factor of 0.977 (determined iteratively), so that the observed and computed 23.8-GHz T_b had a slope of exactly 1.0. (This radiosonde scale factor implies that these nighttime radiosondes had a 2.3% moist bias relative to the MWR, which is consistent with other analyses of RS92 data sets [41], [42].) The bias offset was then computed from the 42 samples that had PWV less than 1.2 cm, yielding an offset value of $0.49\text{ K} \pm 0.08\text{ K}$. This bias offset was then removed from the 23.8-GHz observations, and PWV was retrieved from this channel using a physical iterative retrieval and the MonoRTM.

The PWV scale factors were then used to scale the water vapor mixing ratio profiles of all of the radiosondes used in the subsequent analysis. As a consistency check, the scaled radiosonde profiles were used to compute downwelling infrared spectral radiance with the line-by-line RT model [(LBLRTM); which uses the same physics as MonoRTM]. The LBLRTM calculations were compared to the observations from the ARM Atmospheric Emitted Radiance Interferometer (AERI) at $11.1\ \mu\text{m}$, and these results were compared against similar comparisons made at the ARM Southern Great Plains (SGP) site (Fig. 2). The comparison of AERI observations and LBLRTM calculations, which is very sensitive to the PWV used in the calculation, has an extensive history at the ARM sites ([26]; details of the AERI and the LBLRTM are given in this reference), and these comparisons have been used to evaluate the accuracy of water vapor observations (e.g., [35]–[37]). Thus, the comparison in Fig. 2 confirms that the approach used in this analysis to correct for the bias in the radiosonde humidity profiles is consistent with earlier ARM analyses.

It should be noted that this approach assumes that the water vapor field near the radiosonde launch site is reasonably horizontally homogeneous in the lowest several kilometers, as the radiosonde will drift with the wind and the microwave radiometers are fixed and staring only in the zenith direction. However, in the Murg Valley during this experiment, there were

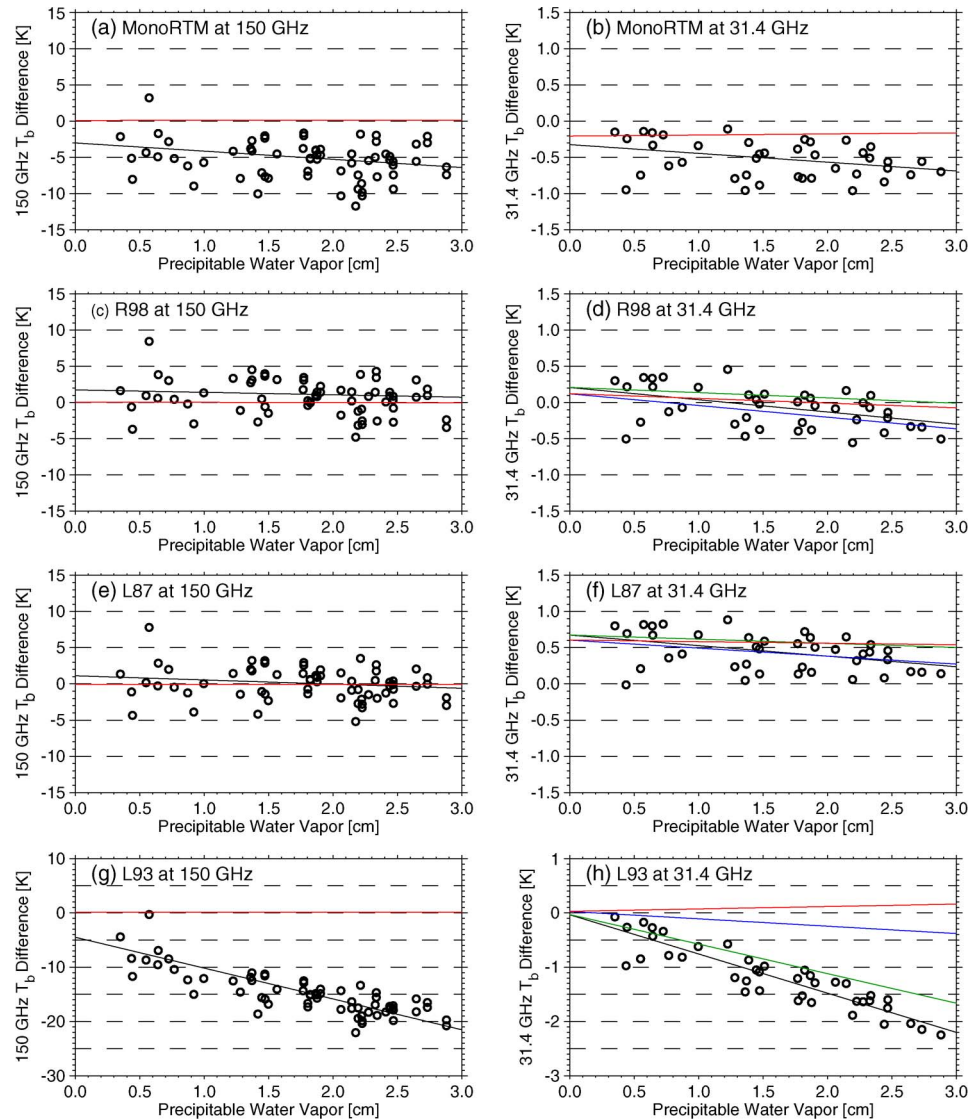


Fig. 3. Observed minus computed T_b differences as a function of PWV at (a), (c), (e), and (g) 150 GHz and (b), (d), (f), and (h) 31.4 GHz for the (a)–(b) MonoRTM, (c)–(d) Rosen98, (e)–(f) Liebe87, and (g)–(h) Liebe93 models. The results from the original models are indicated with the dots with the black lines indicating the regression line fit to these data. For the 150-GHz results, the red lines show the change in the regression when the models are modified to include the updated water vapor continuum. For the 31.4-GHz results, the regression lines for the improvements that result from (green) the updated 22.2-GHz line parameters, (blue) the updated water vapor continuum, and (red) the updated 22.2-GHz line parameters plus the water vapor continuum are shown. The red regression line in panel (b) is for the modified model that has only the water vapor continuum updated. The slopes and intercepts associated with these regression lines are provided in Tables III and VI for 150 and 31.4 GHz, respectively. Note that the y -axis scales for the Liebe93 results are different from the other models. Note that a PWV of 3 cm corresponds to approximately 160 and 23 K at 150 and 31.4 GHz, respectively.

some cases with significant inhomogeneities in the water vapor field [43], but these situations were mitigated by removing cases with standard deviations of the 150-GHz T_b observations larger than 1.5 K in the 40-min window centered around the radiosonde launch time.

These scaled radiosonde humidity profiles were then input into the four different microwave RT models. In window channels such as 150 and 31.4 GHz, the sensitivity to the vertical layering is negligible, particularly since each radiosonde profile contained measurements at thousands of levels. Each radiosonde used in this analysis needed to reach at least 15 km, and the midlatitude summer profile was spliced to the top to extend these profiles through the stratosphere (although the impact on the calculation due to the choice of profile to use in the stratosphere is also negligible).

V. RESULTS

A. Modifying the Water Vapor Continuum Absorption Models

The comparison of the observed and computed brightness temperatures at 150 GHz, where the observed values are the average of all available observations from the two radiometers within the time window, for these 71 cases for the four models are shown in Fig. 3 (black circles and black regression lines), with the statistics provided in Table III. The observed minus calculated residuals for all four models show a dependence on PWV, with the calculated T_b 's becoming increasingly larger than the observations as the PWV increases. The Liebe87, Liebe93, Rosen98, and MonoRTM models show biases relative to the observations of 0.05, -14.87 , 0.74, and -5.35 K, respectively. The residuals using the Liebe93 model show the worst

TABLE III
STATISTICS OF THE OBSERVED MINUS CALCULATED RESIDUALS AT 150 GHz AS A FUNCTION OF PWV, WHERE COMPUTATIONS WERE MADE WITH THE ORIGINAL AND MODIFIED MODELS. "MOD-C" INDICATES THAT ONLY THE WATER VAPOR CONTINUUM COEFFICIENTS WERE MODIFIED. THERE ARE 71 CASES INCLUDED IN THESE STATISTICS

Model	Comment	Slope [K / cm]	Intercept [K]	Bias [K]	RMS [K]
Rosen98	Original	-0.34	1.76	0.74	2.52
	Mod-C	-0.03	0.08	-0.32	2.42
MonoRTM	Original	-1.13	-2.99	-5.35	5.97
	Mod-C	0.01	0.12	-0.20	2.45
Liebe87	Original	-0.57	1.12	0.05	2.23
	Mod-C	0.00	-0.06	-0.10	2.30
Liebe93	Original	-5.68	-4.50	-14.87	15.38
	Mod-C	0.00	0.11	0.16	2.24

RMS: root mean square difference. The uncertainty in the slope and intercept values are approximately 0.06 K/cm and 0.09 K, respectively.

dependence with PWV and a much larger mean bias than the other models. Because the DPR and MWRHF were calibrated independently and show agreement with a bias of 0.12 K and an rms difference of 1.3 K, we conservatively estimate the uncertainty in the 150-GHz observations to be approximately 1.5 K. Thus, the MonoRTM and Liebe93 results are clearly outside the uncertainty of the observations. Previous ground-based work [15] at 150 GHz demonstrated biases of 0.98, -10.37, and 2.00 K for the Liebe87, Liebe93, and Rosen98 models, respectively, and airborne results at 157 GHz [18] showed biases (when the PWV was 1.22 cm, which was close to our mean PWV) of -1.8, -15.6, -0.3, and -4.3 K for the Liebe87, Liebe93, Rosen98, and MonoRTM models, respectively. Thus, our results (Table III) agree well with [15] and [18] given the assumed 1.5-K uncertainty in our observations. Furthermore, the results in [15] and [18] used microwave radiometers that had totally different design and calibration than the DPR and MWRHF, as well as significantly different PWV ranges (the PWV range in [15] was 0.31 to 1.87 cm versus 0.35 to 2.88 cm in this paper).

One possibility is that the differences between the models and the observations are not induced by differences in the treatment of water vapor in the models. To investigate this, we computed the downwelling radiance using these models with no water vapor included, and thus, the radiance was essentially just the emission from oxygen and nitrogen. The differences between the three models relative to each other at 150 GHz were less than 0.7 K, and thus, differences in the dry air absorption between the models do not explain the differences in the bias.

We adjusted the strength of both the self- and foreign-broadened water vapor continuum in the MonoRTM, Rosen98, and Liebe87 models by finding multipliers to C_s and C_f that result in a near zero bias (absolute value less than 0.1 K) and no significant slope (absolute value less than 0.1) between the 150-GHz residuals and PWV. These multipliers and their uncertainties are provided in Table IV. As the Liebe93 model uses a "pseudoline" at 1780 GHz to account for the water vapor continuum absorption, we modified the parameters of this line (strength, air-broadened width, and ratio of the self- to air-broadened width) to match the observations at 150 GHz; these adjustments are provided in Table V. The application of the multipliers, which were derived from the 150-GHz observations, greatly reduced the spread of the C_f and C_s coefficients

TABLE IV
MULTIPLIERS APPLIED TO THE SELF-BROADENED (C_s) AND FOREIGN-BROADENED (C_f) WATER VAPOR CONTINUUM COEFFICIENTS, AS DERIVED FROM THE ANALYSIS OF THE 150-GHz OBSERVATIONS. THE UNCERTAINTY IN THE MULTIPLIERS WAS DETERMINED, ASSUMING A 1.5-K BIAS UNCERTAINTY IN THE OBSERVATIONS AND THE 0.08-K UNCERTAINTY IN THE T_b OFFSET AT 23.8 GHz (IN PARENTHESES, RESPECTIVELY)

Model	C_f multiplier	C_s multiplier
Rosen98	1.105 ± (0.098, 0.030)	0.79 ± (0.17, 0.06)
MonoRTM	0.835 ± (0.073, 0.018)	1.44 ± (0.29, 0.09)
Liebe87	1.090 ± (0.124, 0.038)	0.80 ± (0.20, 0.07)

TABLE V
MULTIPLIERS USED TO SCALE THE LINE PARAMETERS OF THE 1780-GHz "PSEUDOLINE" USED IN L93 TO ACCOUNT FOR WATER VAPOR CONTINUUM ABSORPTION

Component	Original Value	Multiplier
Strength	2230.0	0.785
Air-broadened width	17.620	1.075
Ratio of self- to air-broadened width	30.500	0.813

used in the MonoRTM, Rosen98, and Liebe87 models by a factor of 2 and 6.5, respectively.

These updated continuum coefficients were then used to modify the models ("Mod-C"), and the calculations were repeated. The statistics for the comparison of the observations and modified model calculations at 150 GHz are provided in Table III. Naturally, since the models were modified using the 150-GHz observations, the slopes and intercepts are very close to zero. Interestingly, the rms differences between the observations and the calculations for all four models are now very similar, with values ranging from 2.24 to 2.45 K, whereas the rms differences ranged from 2.23 to 15.38 K with the original unmodified models.

The relative modifications of C_f and C_s in the MonoRTM are supported by [30] and [31], which suggested that C_f needed to be decreased about 30% and C_s increased by a factor of three to come into better agreement with Rosen98 results. English *et al.* [44] indicated that the self-broadened water vapor continuum absorption in the Liebe87 model needed to be increased to improve the comparison with their airborne observations at 157 GHz. However, increasing the strength of the self-broadened component would require a decrease in the foreign-broadened component in order to keep the residual

TABLE VI

SAME AS TABLE III, EXCEPT FOR 31.4 GHz. "MOD-22" INDICATES THAT ONLY THE LINE PARAMETERS (STRENGTH AND WIDTH) OF THE 22.2-GHz LINE WERE MODIFIED. "MOD-22C" INDICATES THAT BOTH THE 22.2-GHz LINE PARAMETERS AND THE WATER VAPOR CONTINUUM WERE MODIFIED

Model	Comment	Slope [K / cm]	Intercept [K]	Bias [K]	RMS [K]
Rosen98	Original	-0.17	0.21	-0.08	0.28
	Mod-C	-0.16	0.12	-0.15	0.30
	Mod-22	-0.07	0.21	0.08	0.26
	Mod-22C	-0.07	0.12	0.03	0.24
MonoRTM	Original	-0.12	-0.32	-0.53	0.59
	Mod-C	0.02	-0.21	-0.20	0.31
Liebe87	Original	-0.15	0.67	0.43	0.50
	Mod-C	-0.11	0.61	0.42	0.48
	Mod-22	-0.06	0.68	0.57	0.62
	Mod-22C	-0.02	0.61	0.56	0.61
Liebe93	Original	-0.72	-0.04	-1.19	1.32
	Mod-C	-0.14	0.03	-0.20	0.32
	Mod-22	-0.54	-0.03	-0.91	1.01
	Mod-22C	0.04	0.03	0.09	0.25

The uncertainty in the slope and intercept values are approximately 0.02 K/cm and 0.03 K, respectively.

between our observations at 150 GHz and the calculations constant with respect to PWV. Kuhn *et al.* [45] have proposed that the C_s in Rosen98 needs to be increased by 17% based on laboratory measurements at 350 GHz (which is in disagreement with our findings), but also suggests that C_f in Rosen98 needs to be increased a similar amount (in general agreement with our findings).

B. Evaluation Using 31.4-GHz Observations

The continuum multipliers in Tables IV and V indicate that significant changes must be made to both the self- and foreign-broadened water vapor continuum coefficients in order to get agreement with the observations at 150 GHz. Assuming that these multipliers are frequency independent, how does this affect the results at other frequencies? To address this, we computed the downwelling brightness temperature at 31.4 GHz with both the original and Mod-C modified models, which were then compared against the yet-unused observation from the two-channel microwave radiometer. For the Rosen98, Liebe87, and Liebe93 models, we also performed calculations with and without the changes to the 22.2-GHz linewidth suggested by [9], where we also changed the strength of the 22.2-GHz line in the Liebe93 model to agree with the strength used in the other three models (which are all within 1% of each other). The results from these different models relative to the observations are provided in Table VI and Fig. 3.

The change in the C_f and C_s coefficients in MonoRTM greatly reduced the magnitude of the slope of the observed minus calculated residuals as a function of PWV [Fig. 3(b)], although there is still a small bias in the data. The 31.4-GHz channel is known to have small biases [40], but the improvement in the slope (i.e., a value closer to zero) suggests that the modified MonoRTM is better than the original version. For the Rosen98 and Liebe87 models [Fig. 3(d) and (f), respectively], the modification to the water vapor continuum (blue regression lines) had a relatively small effect at 31.4 GHz, but the change to the half width of the 22.2-GHz line (red regression line) greatly improved these models relative to the observations (by making slope closer to zero). The combined

changes of the width of the 22.2-GHz line and the water vapor continuum for these two models are not significantly different than just the change of the 22.2-line parameters, and thus, this is not a conclusive test on the accuracy of the water vapor continuum multipliers. Finally, the Liebe93 model [Fig. 3(h)] is substantially improved by both the change to the 22.2-GHz line parameters (strength and widths for this model) and the water vapor continuum adjustment, with the significant PWV dependence of the observed minus calculated residuals largely removed. The Mod-22C Liebe93, Mod-C MonoRTM, and Mod-22C Rosen98 models (continuum and 22-GHz line adjustments) decreased the bias and the rms difference with the observations and improved in the slope relative to the original models, thereby suggesting that these modified models are better than the original versions. However, the results for the Liebe87 model are inconclusive as to whether any of the modified models is significantly better than the original.

Our results here are based upon a midlatitude site with PWV that ranged from 0.35 to 2.88 cm. This data set does not fully test the quadratic dependence of the self-broadened water vapor continuum on water vapor, nor does it adequately test the temperature dependence of the continuum coefficients used in the models. Thus, a more detailed look is needed at both the linewidth and the continuum, over a wide range of atmospheric conditions with spectrally resolved observations. The contribution from the linewidth (from either the 22.2- or 183.3-GHz water vapor lines) is relatively small at 150 GHz, compared to 31.4 GHz.

C. Impact Across the Microwave Spectrum

Observations at 150 GHz were used to characterize four often-used absorption models. We have shown that scaling the self- and foreign-broadened water vapor continuum coefficients is needed to get agreement with these observations and that better agreement is achieved at 31.4 GHz if both the water vapor continuum is scaled and the parameters of the 22.2-GHz line are updated to agree with [9]. A natural question is how do these modified models compare relative to each other across the spectrum? To get a better sense of the spectral differences between

TABLE VII
PWV, MEAN RADIATING TEMPERATURE AT 23.8 GHz (T_{MR}),
AND SURFACE PRESSURE (P_{sfc}) FOR THE SIX
“CLIMATOLOGICAL” RADIOSONDES

Site	PWV [cm]	T_{MR} [K]	P_{sfc} [mb]
Payerne	0.55	259.8	947
Payerne	1.96	278.0	960
Payerne	3.69	285.9	964
Darwin	1.93	292.6	1010
Darwin	3.74	292.8	1011
Darwin	6.40	292.3	1003

the four models, we selected six “climatological” radiosonde profiles that span a wide range of water vapor and temperature conditions, with three radiosondes selected from both midlatitude (Payerne, Switzerland) and tropical (Darwin, Australia) sites (Table VII). These profiles were selected such that the two wetter cases from Payerne had similar PWV to the two drier cases from Darwin so that the temperature dependence differences between the models could be seen. The spectral downwelling brightness temperature was then computed for each of the climatological radiosondes for the different original and modified models.

The differences between the original and modified versions of the same model are shown in Fig. 4. The change to the MonoRTM [Fig. 4(a)] is very significant for the drier cases, and there is relatively little difference across the spectrum when the PWV is large. The modifications to the Rosen98 [Fig. 4(b)] and Liebe87 [Fig. 4(c)] models are largest in the 60–180-GHz range when the PWV is large, but the differences are largest in the 180–380-GHz range when the PWV is small. The Liebe93 model [Fig. 4(d)] shows very significant differences across the entire spectrum where, similar to the Liebe87 and Rosen98 models, the difference between the original and modified models per PWV changes with frequency. These differences, particularly in windows used for remote sensing of cloud or surface properties (e.g., at 90 GHz), are significant for all four models, and because of the PWV dependence, understanding the impact of these modifications on other remote sensing applications is difficult.

The original models differed significantly from each other, as shown in Fig. 5, where the MonoRTM was used as the baseline. Differences as large as 5–15 K exist between different models, and the differences depend on both the frequency and PWV. The differences in the temperature dependences between different models are also seen, as the curves that have the same PWVs from the midlatitudes versus tropics are distinctly separated [e.g., the 1.9-cm soundings for the Liebe87 and MonoRTM models in Fig. 5(c)].

Fig. 6 shows the downwelling brightness temperature for these same six cases when the best version of each modified model was used (Mod-C for MonoRTM and Mod-22C for Rosen98, Liebe87, and Liebe93). Immediately, we can see that the modified MonoRTM and Rosen98 models are in much better agreement, with differences in all of the atmospheric windows being less than 2 K. Similarly, the modified MonoRTM and the Liebe87 models are also in much better agreement in the atmospheric windows, particularly for the three midlatitude (Payerne) radiosondes. However, the differences between these two models for the tropical cases are due to the differences

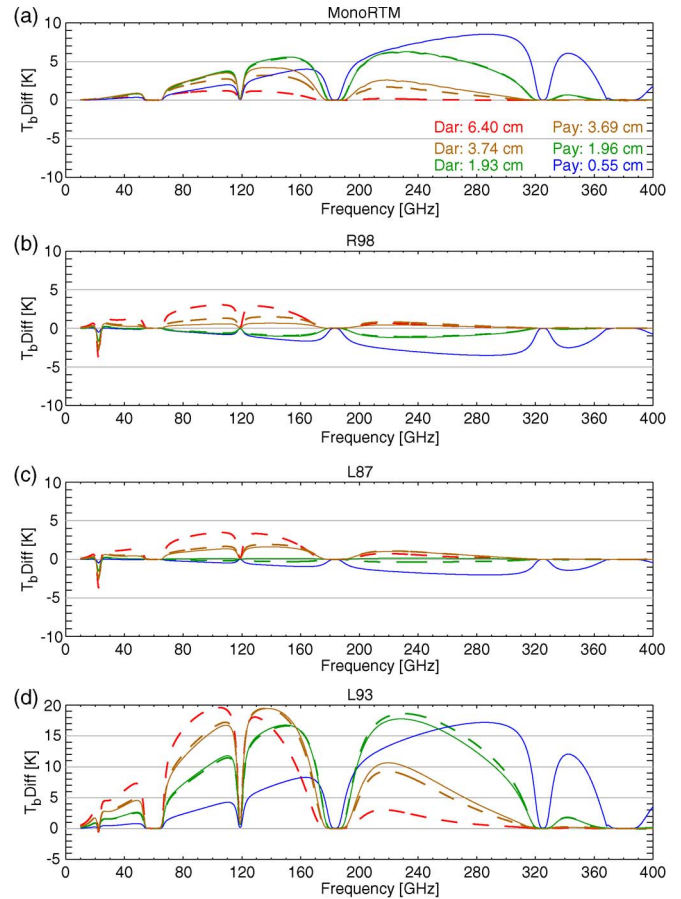


Fig. 4. Downwelling spectral brightness temperature difference for the original minus modified models from 10 to 400 GHz computed using the (a) MonoRTM, (b) Rosen98, (c) Liebe87, and (d) Liebe93 models. The modified models used here are the Mod-C for MonoRTM and Mod-22C for the other three. The spectra computed using the midlatitude profiles are shown with solid lines, while the tropical data are denoted with dashed lines. The colors correspond to different amounts of PWV. Note that the scale of the y -axis in panel (d) is larger than in panels (a), (b), and (c). The magnitude of the MonoRTM brightness temperature spectra for the six profiles is shown in Fig. 5(a).

in the temperature dependence of the water vapor continuum absorption. Recent theoretical results from Ma and Tipping [46] suggest that the temperature dependence of the foreign-broadened water vapor continuum is closer to the Liebe93 value of 4.55 (and, hence, the values used by Rosen98 and MonoRTM) than the Liebe87 value of 7.5. The differences between the MonoRTM and Liebe93 are also significantly improved, although there are some significant differences between 60 and 120 GHz associated with the absorption due to oxygen. There are also some differences between the MonoRTM and Liebe93 for the driest midlatitude case [solid blue line in Fig. 6(d)], as well as for the driest tropical case (dashed green line). Finally, the modified Liebe87 and Liebe93 models, and, to a lesser degree, the modified Rosen98 model, show differences with the modified MonoRTM around the 183.3-GHz water vapor line, particularly when the PWV is small; this was expected because of the incorporation of improved spectroscopy of this absorption line [33].

VI. CONCLUSION

We have utilized the downwelling brightness temperature observations at 150 GHz from two independently calibrated

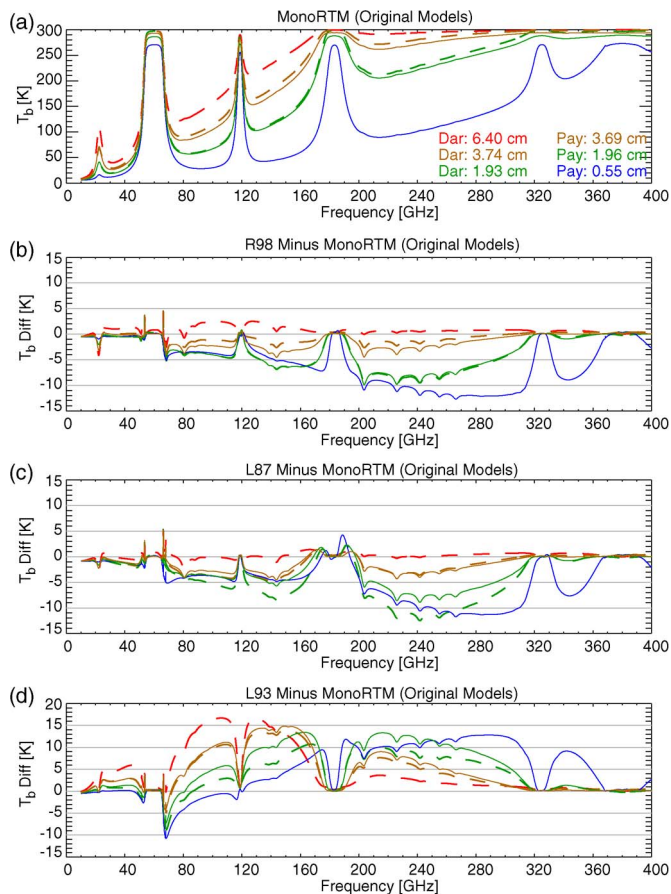


Fig. 5. Downwelling spectral brightness temperature from 10 to 400 GHz computed using (a) the original MonoRTM and the spectral differences for (b)–(d) the original Rosen98, Liebe87, and Liebe93 models relative to the MonoRTM. The spectra computed using the midlatitude profiles are shown with solid lines, while the tropical data are denoted with dashed lines. The colors correspond to different amounts of PWV. Note that the scale of the y -axis in panel (d) is larger than in panels (b) and (c).

microwave radiometers deployed at a midlatitude continental site to evaluate four different microwave absorption models in a clear-sky atmosphere. The agreement between these two radiometers was very good (approximately 1.5 K). From these observations, we propose that the strength of the foreign- and self-broadened water vapor continuum absorption should be significantly modified in all four of the microwave RT models. These modified models were then compared to observations at 31.4 GHz to evaluate the improvement relative to the original models. The Rosen98, Liebe87, and Liebe93 models were also modified to use updated line parameters for the 22.2-GHz water vapor line.

The 31.4-GHz closure results demonstrate that the modified MonoRTM, Rosen98, and Liebe93 models are improved relative to the original models. However, the 31.4-GHz results are inconclusive about whether the modifications made to the Liebe87 model do indeed lead to better results at this frequency. The self-broadened continuum absorption is proportional to the square of the water vapor (3), (5); however, due to the scatter in the data (Fig. 3), as well as the limited range of PWV (0.35 to 2.88 cm), there is too much uncertainty in the fits to determine if the multipliers in Table IV are indeed keeping the observed minus computed residuals linear with PWV or inducing curvature as the PWV gets larger. A significant limitation of this

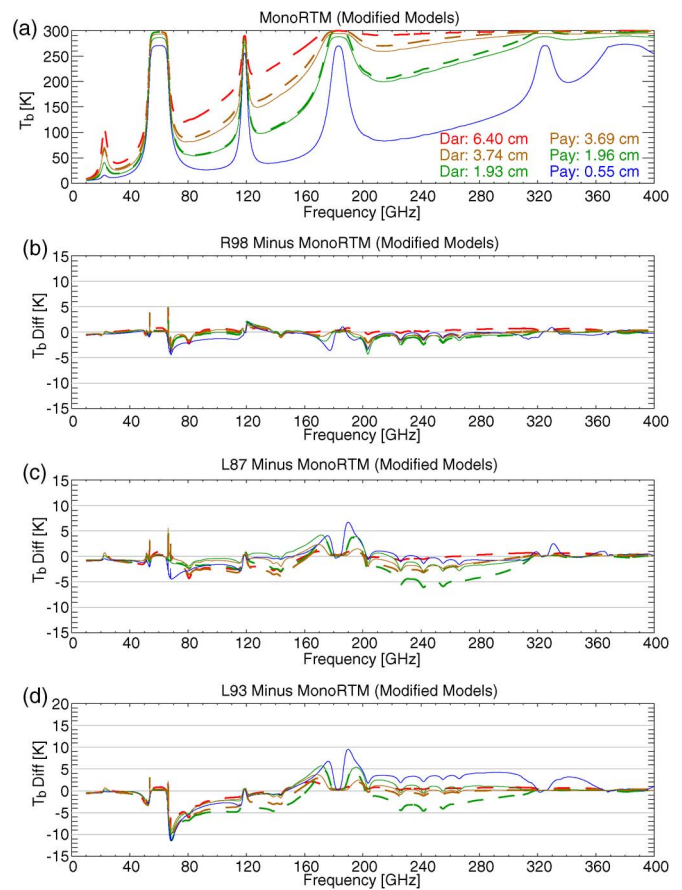


Fig. 6. Same as Fig. 5, except using the modified models (Mod-C for MonoRTM and Mod-22C for the other three models). Again, the scale of the y -axis in panel (d) is different from panels (b) and (c).

data set is that the maximum PWV is less than 3 cm; a larger range of PWV with some significantly higher values is needed to really evaluate whether the hypothesized change to the C_s and C_f coefficients is accurate.

We have evaluated these models relative to each other across the entire microwave spectral range using a small set of radiosondes chosen to span a wide range of PWV and temperature. The results (Figs. 5 and 6) demonstrate that the modified models are in much better agreement with each other, with the differences between the MonoRTM and Rosen98 models being within 2 K over almost the entire spectral range from 10 to 400 GHz. These model-versus-model comparisons demonstrate that there are differences in the assumed temperature dependence of the water vapor continuum absorption, which lead to differences between models of nearly 5 K (e.g., at 150 and 220 GHz between the modified MonoRTM and Liebe87 models). The model-versus-model results are unable to indicate which model is more correct, and unfortunately, the range of temperatures experienced at the AMF site does not allow for an adequate investigation of the temperature dependence of the absorption at 150 GHz. There are also significant differences between the different models associated with oxygen absorption between 60 and 120 GHz and the 183.3-GHz water vapor line parameters.

An additional data set that covers a wider range of PWV conditions (particularly some moister cases) and a large range of temperature conditions is needed to further validate the

proposed water vapor continuum multipliers. Accurate well-characterized measurements are also needed at additional frequencies to evaluate whether or not these multipliers are frequency independent.

One strong conclusion from this study is that the original Liebe93 model does not match the observations at 150 or 31.4 GHz; this conclusion is supported by the analyses at different frequencies (e.g., [15]). Unfortunately, many groups are still using the water vapor continuum model from this model (i.e., the models in the intercomparison study of [16]).

REFERENCES

- [1] L. S. Rothman, L. S. Rothman, D. Jacquemart, A. Barbe, D. Chris Benner, M. Birk, L. R. Brown, M. R. Carleer, C. Chackerian, Jr., K. Chance, L. H. Coudert, V. Dana, V. M. Devi, J.-M. Flaud, R. R. Gamache, A. Goldman, J.-M. Hartmann, K. W. Jucks, A. G. Maki, J.-Y. Mandin, S. T. Massie, J. Orphal, A. Perrin, C. P. Rinsland, M. A. H. Smith, J. Tennyson, R. N. Tolchenov, R. A. Toth, J. Vander Auwera, P. Varanasi, and G. Wagner, "The HITRAN 2004 molecular spectroscopic database," *J. Quant. Spectrosc. Radiat. Transf.*, vol. 96, no. 2, pp. 139–204, Dec. 2005.
- [2] T. J. Hewison, "1D-VAR retrieval of temperature and humidity profiles from a ground-based microwave radiometer," *IEEE Trans. Geosci. Remote Sens.*, vol. 45, no. 7, pp. 2163–2168, Jul. 2007.
- [3] S. Crewell and U. Löhnert, "Accuracy of boundary layer temperature profiles retrieved with multifrequency multiangle microwave radiometry," *IEEE Trans. Geosci. Remote Sens.*, vol. 45, no. 7, pp. 2195–2201, Jul. 2007.
- [4] Q. Fu, C. M. Johanson, J. M. Wallace, and T. Reichler, "Enhanced mid-tropospheric warming in satellite measurements," *Science*, vol. 312, no. 5777, p. 1179, May 2006.
- [5] E. R. Westwater, Y. Han, M. D. Shupe, and S. Y. Matrosov, "Analysis of integrated cloud liquid and precipitable water vapor retrievals from microwave radiometers during the Surface Heat Budget of the Arctic Ocean project," *J. Geophys. Res.*, vol. 106, no. D23, pp. 32019–32030, 2001.
- [6] D. Cimini, E. R. Westwater, A. J. Gasiewski, M. Klein, V. Y. Leuski, and J. C. Liljgren, "Ground-based millimeter- and submillimeter-wave observations of low vapor and liquid water contents," *IEEE Trans. Geosci. Remote Sens.*, vol. 45, no. 7, pp. 2169–2180, Jul. 2007.
- [7] C. Melsheimer and G. Heygster, "Improved retrieval of total water vapor over polar regions from AMSU-B microwave radiometer data," *IEEE Trans. Geosci. Remote Sens.*, vol. 46, no. 8, pp. 2307–2322, Aug. 2008.
- [8] U. Löhnert, D. D. Turner, and S. Crewell, "Ground-based temperature and humidity profiling using spectral infrared and microwave observations: Part 1. Retrieval performance in clear sky conditions," *J. Appl. Meteorol. Clim.*, vol. 48, pp. 1017–1032, May 2009. DOI: 10.1175/2008JAMC2060.1.
- [9] J. C. Liljgren, S. A. Boukabara, K. Cady-Pereira, and S. A. Clough, "Effect of the half-width of the 22.2 GHz water vapor line on retrievals of temperature and water vapor profiles with a twelve channel microwave radiometer," *IEEE Trans. Geosci. Remote Sens.*, vol. 43, no. 5, pp. 1102–1108, May 2005.
- [10] C. Prigent, E. Jaumouille, F. Chevallier, and F. Aires, "A parameterization of the microwave land surface emissivity between 19 and 100 GHz, anchored to satellite-derived estimates," *IEEE Trans. Geosci. Remote Sens.*, vol. 46, no. 2, pp. 344–352, Feb. 2008.
- [11] N. C. Grody and F. Weng, "Microwave emission and scattering from deserts: Theory compared with satellite measurements," *IEEE Trans. Geosci. Remote Sens.*, vol. 46, no. 2, pp. 361–375, Feb. 2008.
- [12] R. Bindlish, T. J. Jackson, A. J. Gasiewski, M. Klein, and E. G. Njoku, "Soil moisture mapping and AMSR-E validation using the PSR in SMEX02," *Remote Sens. Environ.*, vol. 103, no. 2, pp. 127–139, Jul. 2006.
- [13] P. Zuidema, E. R. Westwater, C. Fairall, and D. Hazen, "Ship-based liquid water path estimates in marine stratocumulus," *J. Geophys. Res.*, vol. 110, no. D20, p. D20 206, Oct. 2005. DOI:10.1029/2005JD005833.
- [14] R. Marchand, T. Ackerman, E. R. Westwater, S. A. Clough, K. Cady-Pereira, and J. C. Liljgren, "An assessment of microwave absorption models and retrievals of cloud liquid water using clear-sky data," *J. Geophys. Res.*, vol. 108, no. D24, pp. AAC7-1–AAC7-11, Dec. 2003.
- [15] T. J. Hewison, D. Cimini, L. Martin, C. Gaffard, and J. Nash, "Validating clear air absorption models using ground-based microwave radiometers and vice-versa," *Meteorol. Z.*, vol. 15, no. 1, pp. 27–36, 2006.
- [16] C. Melsheimer, C. Verdes, S. A. Buehler, C. Emde, P. Eriksson, D. G. Feist, S. Ichizawa, V. O. John, Y. Kasai, G. Kopp, N. Koulev, N. Koulev, O. Lemke, S. Ochiai, F. Schreier, F. Schreier, M. Suzuki, C. Takahashi, S. Tsujimaru, and J. Urban, "Intercomparison of general purpose clear sky atmospheric radiative transfer models for the millimeter/submillimeter spectral range," *Radio Sci.*, vol. 40, no. 1, pp. RS1 007.1–RS1 007.28, Feb. 2005.
- [17] P. E. Racette, E. J. Kim, J. R. Wang, E. R. Westwater, M. Klein, V. Leuski, Y. Han, A. J. Gasiewski, D. Cimini, D. C. Jones, W. Manning, and P. Kiedron, "Measurement of low amounts of precipitable water vapor using ground-based millimeterwave radiometry," *J. Atmos. Ocean. Technol.*, vol. 22, no. 4, pp. 317–337, Apr. 2005.
- [18] T. J. Hewison, "Aircraft validation of clear air absorption models at millimeter wavelengths (89–183 GHz)," *J. Geophys. Res.*, vol. 111, no. D14, pp. D14 303.1–D14 303.11, Jul. 2006.
- [19] V. Wulfmeyer, A. Behrendt, H.-S. Bauer, C. Kottmeier, U. Corsmeier, A. Blyth, G. Craig, U. Schumann, M. Hagen, S. Crewell, P. Di Girolamo, C. Flamant, M. Miller, A. Montani, S. Mobbs, E. Richard, M. W. Rotach, M. Arpagaus, H. Russchenberg, P. Schlüssel, M. König, V. Gärtner, R. Steinacker, M. Dorninger, D. D. Turner, T. Weckwerth, A. Hense, and C. Simmer, "The convective and orographically induced precipitation study: A research and development project of the World Weather Research Program for improving quantitative precipitation forecasting in low-mountain regions," *Bull. Amer. Meteorol. Soc.*, vol. 89, no. 10, pp. 1477–1486, Oct. 2008.
- [20] S. Crewell, M. Mech, T. Reinhardt, C. Selbach, H.-D. Betz, E. Brocard, G. Dick, E. O'Connor, J. Fischer, T. Hanisch, T. Hauf, A. Hunerbein, L. Delobbe, A. Mathes, G. Peters, H. Wernli, M. Wiegner, and V. Wulfmeyer, "The general observation period 2007 within the priority program on quantitative precipitation forecasting: Concept and first results," *Meteor. Z.*, vol. 17, no. 6, pp. 849–866, 2008.
- [21] M. Miller and A. Slingo, "The ARM mobile facility and its first international deployment: Measuring radiative flux divergence in West Africa," *Bull. Amer. Meteorol. Soc.*, vol. 88, no. 8, pp. 1229–1244, Aug. 2007.
- [22] S. Crewell and U. Löhnert, "Accuracy of cloud liquid water path from ground-based microwave radiometry. Part II, sensor accuracy and synergy," *Radio Sci.*, vol. 38, no. 3, p. 8042, 2003. DOI:10.1029/2002RS002634.
- [23] D. D. Turner, A. M. Vogelmann, R. T. Austin, J. C. Barnard, K. Cady-Pereira, J. C. Chiu, S. A. Clough, C. Flynn, M. M. Khaiyer, J. Liljgren, K. Johnson, B. Lin, C. Long, A. Marshak, S. Y. Matrosov, S. A. McFarlane, M. Miller, Q. Min, P. Minnis, W. O'Hirok, Z. Wang, and W. Wiscombe, "Thin liquid water clouds: Their importance and our challenge," *Bull. Amer. Meteorol. Soc.*, vol. 88, no. 2, pp. 177–190, Feb. 2007.
- [24] T. Rose, S. Crewell, U. Löhnert, and C. Simmer, "A network suitable microwave radiometer for operational monitoring of the cloudy atmosphere," *Atmos. Res.*, vol. 75, no. 3, pp. 183–200, May 2005.
- [25] Y. Han and E. R. Westwater, "Analysis and improvement of tipping calibration for ground-based microwave radiometers," *IEEE Trans. Geosci. Remote Sens.*, vol. 38, no. 3, pp. 43–52, May 2000.
- [26] D. D. Turner, D. C. Tobin, S. A. Clough, P. D. Brown, R. G. Ellingson, E. J. Mlawer, R. O. Knuteson, H. E. Revercomb, T. R. Shippert, and W. L. Smith, "The QME AERI LBLRTM: A closure experiment for downwelling high spectral resolution infrared radiance," *J. Atmos. Sci.*, vol. 61, no. 22, pp. 2657–2675, Nov. 2004.
- [27] J. C. Liljgren, "Automatic self-calibration of ARM microwave radiometers," in *Microwave Radiometry and Remote Sensing of the Earth's Surface and Atmosphere*, P. Pampaloni and S. Paloscia, Eds. Utrecht, The Netherlands: VSP Press, 2000, pp. 433–443.
- [28] H. J. Liebe and D. H. Layton, "Millimeter-wave properties of the atmosphere: Laboratory studies and propagation modeling," *Nat. Telecommun. Inf. Admin.*, Boulder, CO, NTIA Rep. 87-224, 1987.
- [29] H. J. Liebe, G. A. Hufford, and M. G. Cotton, "Propagation modeling of moist air and suspended water/ice particles at frequencies below 1000 GHz," presented at the AGARD 52nd Specialists Meeting Electromagnetic Wave Propagation Pane, Palma de Mallorca, Spain, May 17–21, 1993, Paper No 3/1-10.
- [30] P. W. Rosenkranz, "Water vapor continuum absorption: A comparison of measurements and models," *Radio Sci.*, vol. 33, no. 4, pp. 919–928, 1998.
- [31] P. W. Rosenkranz, "Correction: 'Water vapor continuum absorption: A comparison of measurements and models'," *Radio Sci.*, vol. 34, no. 4, p. 1025, 1999.
- [32] S. A. Clough, M. W. Shephard, E. J. Mlawer, J. S. Delamere, M. J. Iacono, K. Cady-Pereira, S. Boukabara, and P. D. Brown, "Atmospheric radiative transfer modeling: A summary of the AER codes," *J. Quant. Spectrosc. Radiat. Transf.*, vol. 91, no. 2, pp. 233–244, Mar. 2005.

- [33] V. H. Payne, J. S. Delamere, K. E. Cady-Pereira, R. R. Gamache, J.-L. Moncet, E. J. Mawer, and S. A. Clough, "Air-broadened half-widths of the 22- and 183-GHz water-vapor lines," *IEEE Trans. Geosci. Remote Sens.*, vol. 46, no. 11, pp. 3601–3617, Nov. 2008.
- [34] S. A. Clough, F. X. Kneizys, and R. W. Davies, "Line shape and the water vapor continuum," *Atmos. Res.*, vol. 23, pp. 229–241, 1989.
- [35] H. E. Revercomb, D. D. Turner, D. C. Tobin, R. O. Knuteson, W. F. Feltz, J. Barnard, J. Bösenberg, S. Clough, D. Cook, R. Ferrare, J. Goldsmith, S. Gutman, R. Halthore, B. Lesht, J. Liljegren, H. Linné, J. Michalsky, V. Morris, W. Porch, S. Richardson, B. Schmid, M. Splitt, T. Van Hove, E. Westwater, and D. Whiteman, "The Atmospheric Radiation Measurement program's water vapor intensive observation periods: Overview, accomplishments, and future challenges," *Bull. Amer. Meteorol. Soc.*, vol. 84, no. 2, pp. 217–236, Feb. 2003.
- [36] D. D. Turner, B. M. Lesht, S. A. Clough, J. C. Liljegren, H. E. Revercomb, and D. C. Tobin, "Dry bias and variability in Vaisala radiosondes: The ARM experience," *J. Atmos. Ocean. Technol.*, vol. 20, no. 1, pp. 117–132, Jan. 2003.
- [37] K. Cady-Pereira, M. W. Shephard, D. D. Turner, E. J. Mlawer, S. A. Clough, and T. J. Wagner, "Improved daytime column-integrated precipitable water vapor from Vaisala radiosonde humidity sensors," *J. Atmos. Ocean. Technol.*, vol. 25, no. 6, pp. 873–883, Jun. 2008.
- [38] H. Vömel, H. Selkirk, L. M. Miloshevich, J. Valverde-Canossa, J. Valdés, E. Kyro, R. Kivi, W. Stolz, G. Peng, and A. Diaz, "Radiation dry bias of the Vaisala RS92 humidity sensor," *J. Atmos. Ocean. Technol.*, vol. 24, no. 6, pp. 953–963, Jun. 2007.
- [39] D. D. Turner, "Improved ground-based liquid water path retrievals using a combined infrared and microwave approach," *J. Geophys. Res.*, vol. 112, no. D15, p. D15204, Aug. 2007. DOI:10.1029/2007JD008530.
- [40] D. D. Turner, S. A. Clough, J. C. Liljegren, E. E. Clothiaux, K. Cady-Pereira, and K. L. Gaustad, "Retrieving liquid water path and precipitable water vapor from Atmospheric Radiation Measurement (ARM) microwave radiometers," *IEEE Trans. Geosci. Remote Sens.*, vol. 45, no. 11, pp. 3680–3690, Nov. 2007.
- [41] L. M. Miloshevich, H. Vömel, D. N. Whiteman, and T. Leblanc, "Accuracy assessment and correction of Vaisala RS92 radiosondes water vapor measurements," *J. Geophys. Res.*, vol. 114, p. D11305, 2009. DOI:10.1029/2008JDO11565.
- [42] D. Cimini, F. Nasir, E. R. Westwater, V. H. Payne, D. D. Turner, E. J. Mlawer, M. L. Exner, and M. Cadetdu, "Comparison of ground-based millimeter-wave observations in the Arctic winter," *IEEE Trans. Geosci. Remote Sens.*, vol. 47, no. 9, pp. 3098–3106, Sep. 2009.
- [43] S. Kneifel, S. Crewell, U. Löhnert, and J. Schween, "Investigating water vapor variability by ground-based microwave radiometry: Evaluation using airborne observations," *IEEE Geosci. Remote Sens. Lett.*, vol. 6, no. 1, pp. 157–161, Jan. 2009.
- [44] S. J. English, C. Guillou, C. Prigent, and D. C. Jones, "Aircraft measurements of water vapor continuum absorption at millimeter wavelengths," *Q. J. R. Meteorol. Soc.*, vol. 120, pp. 603–625, 1994.
- [45] T. Kuhn, A. Bauer, M. Godon, S. Bühler, and K. , "Water vapor continuum: Absorption measurements at 350 GHz and model calculations," *J. Quant. Spectrosc. Radiat. Transf.*, vol. 74, no. 5, pp. 545–562, Sep. 2002.
- [46] Q. Ma and R. H. Tipping, "A simple analytical parameterization for the water vapor millimeter wave foreign continuum," *J. Quant. Spectrosc. Radiat. Transf.*, vol. 82, no. 1–4, pp. 517–531, Nov./Dec. 2003.



David D. Turner received the B.A. and M.S. degrees in mathematics from Eastern Washington University, Cheney, in 1992 and 1994, respectively, and the Ph.D. degree in atmospheric science from the University of Wisconsin, Madison, in 2003.

He is currently a Researcher with the Space Science and Engineering Center, University of Wisconsin. He is actively involved in the Department of Energy's Atmospheric Radiation Measurement (ARM) program and is currently the Chair of the ARM Radiative Processes working group and is a

Member of the ARM Science Team Executive Committee. His current research interests include infrared and microwave remote sensing; long wave radiative transfer in clear and cloudy atmospheres; and retrieving water vapor, cloud, and aerosol properties from active and passive remote sensors.

Dr. Turner is a member of the American Meteorological Society and the American Geophysical Union.

Maria P. Cadetdu received the Laurea degree in physics from the University of Cagliari, Cagliari, Italy, in 1994 and the Ph.D. degree in physics from Heriot-Watt University, Edinburgh, U.K., in 2002.

Since 2005, she has been with the Argonne National Laboratory where her primary duty has been as the Instrument Mentor for the U.S. Department of Energy Atmospheric Radiation Measurement Program microwave radiometer instrumentation. Her research interests include microwave radiometers and application of remote sensing to atmospheric research.

Dr. Cadetdu is a member of the American Geophysical Union.



Ulrich Löhnert received the Ph.D. degree in meteorology from the University of Bonn, Bonn, Germany, in 2002.

From 1998 to 2003, he was a Research Scientist with the Universities of Bonn and Kiel, Germany, and also with the Environmental Technology Laboratory, National Oceanic Atmospheric Administration. From 2004 to 2006, he was an Assistant Professor with the Ludwig-Maximilians-University of Munich, Munich, Germany. He is currently with the Institute of Geophysics and Meteorology, University of

Cologne, Cologne, Germany. Recently, his research has focused on the development of statistical and physical methods for deriving profiles of the atmospheric thermodynamic state through sensor synergy, as well as on the retrieval of ice microphysical properties.



Susanne Crewell (M'06) received the Ph.D. degree in physics from the University of Bremen, Bremen, Germany, in 1993.

From 1994 to 1996, she was with the State University of New York, Stony Brook. After two years at the Ludwig-Maximilians-University of Munich, Munich, Germany, as a Professor of experimental meteorology, she is currently with the Institute of Geophysics and Meteorology, University of Cologne, Cologne, Germany. Her research interest focuses on passive microwave remote sensing of the

Earth. She has worked on latent heat flux determination from satellite, observation of stratospheric trace gases from aircraft and ground, and tropospheric water vapor, temperature, and hydrometeors. Her current main interests include the combination of observations in different spectral regions and the use of observations for improving atmospheric weather forecast models.

Dr. Crewell is an Associate Editor of the IEEE GEOSCIENCE AND REMOTE SENSING LETTERS.



Andrew M. Vogelmann was born in Burlington, VT, in 1962. He received the B.S. degree in physics from the University of Vermont, Burlington, in 1984, the M.S. degree in meteorology from the University of Maryland, College Park, in 1986, and the Ph.D. degree in meteorology from The Pennsylvania State University, University Park, in 1994.

He was with the Scripps Institution of Oceanography from 1995 to 2003. He has been a Scientist with the Atmospheric Sciences Division, Brookhaven National Laboratory, Upton, NY, since 2003. His research

has been concerned with climate and the Earth's energy balance through a combination of observational and modeling studies of cloud- and aerosol-radiative interactions, and remote sensing. He has authored or coauthored 20 peer-reviewed journal articles. He has been involved with the U.S. Department of Energy's Atmospheric Radiation Measurement Program since 1995 and has served as an Associate Chief Scientist for the program since 2006.